Characterization and application of temperature microoptodes for use in aquatic biology

Gerhard Holst, Michael Kühl, Ingo Klimant, Gregor Liebsch and Oliver Kohls

Max-Planck-Institute for Marine Microbiology, Microsensor Research Group, Celsiusstr. 1,
D-28359 Bremen, Germany
IK, GL Institute for Analytical Chemistry, University of Regensburg,
D-93040 Regensburg, Germany

Abstract

Benthic aquatic environments like biofilms or sediments are often investigated by measuring profiles of chemical or physical parameters at a high spatial resolution (< 50 µm). This is necessary to understand e.g. transport processes and the biogeochemistry of the sediment water interface. A variety of electrochemical and optical microsensors has been developed and used for this purpose. In most of these applications the temperature of the investigated biofilms or sediments is assumed to be constant. However measurements with thermocouples of an appr. diameter of 300 µm have shown that this is not always the case for illuminated shallow water sediments and biofilms. We developed new microoptodes for measuring temperature distributions at a high spatial (< 50 µm) and thermal (< 0.2 °C) resolution in aquatic systems.
The new sensors are based on a flurophore that is well known for its application in oxygen sensing - Ruthenium(II)-tris-1,10-phenantroline. Demas et al. (1992) discussed the possible use of highly luminescent transition metal complexes as temperature indicators. We have approached this idea from our experiences with ruthenium complexes as oxygen indicators. The first realized sensor consists of a closed microcapillary filled with an indicator solution and an inserted tapered optical fiber. The principle uses the temperature dependence of the fluorescence lifetime in the solution. To keep the solution oxygen free an oxygen scavenger is added to it. The change of the lifetime is detected by a special measuring device that uses a phase modulation technique.

Keywords: temperature microoptode, fiber optic sensor, fibre optic sensor, phase modulation, temperature microsensor, luminescence sensor, luminescence lifetime

1 Introduction

The investigation of the metabolism of algae and bacteria that live in the water-sediment interface in marine environments is often performed by use of microsensors. These sensors can measure the steep gradients of solute concentrations that may occur over few hundreds of micrometers in these systems. Normally, the temperature along the measured concentration profiles is assumed to be constant. This assumption seems justified for sediments in deeper waters but for intertidal sediments or shallow water systems, exposed to solar radiation, temperature gradients may be of importance. Fine scale temperature measurements in these communities have so far been limited by the availability of temperature microsensors.
We developed optical temperature microsensors with the goal of reaching a spatial resolution of < 100 µm and a thermal resolution of better than 0.25 °C in the range of 0 - 50 °C.

2 Optical temperature microsensor

2.1 Sensing scheme and indicators

The sensing scheme is based on the temperature dependence of some of the oxygen indicators [1, 2, 10] that we use for our oxygen microoptodes [8-10]. Either the temperature dependence of the zero oxygen lifetime or the temperature dependence of the quenching coefficient can be used for

SPIE Vol. 2980 • 0277-786X/97/$10.00

temperature sensing. The possible use of ruthenium complexes was proposed by Demas and DeGraff [1]. One of the most temperature sensitive dyes of these complexes is the tris(1,10-phenantroline)-ruthenium(II)-complex (table I) [2], that only has one disadvantage, its short lifetime of a few hundred nanoseconds. Another dye that has a highly temperature dependent quenching coefficient is the Platinum(II) meso-tetra (pentafluorophenyl) porphine that is also used for oxygen sensing (table I). It has a lifetime in the range of ~ 20 - 50 µs.
We immobilized the indicators in such a way that they were either not or only weakly sensitive to oxygen, or we kept the oxygen concentration constant. The following different approaches were tested:

sensor type	indicator	matrix	λ_{ex} / λ_{em} [nm]
[A]	(1) Tris(1,10-phenantroline)-ruthenium(II)-complex [RuPhe]	micellar dissolved in a solution of sodium dodecylsulfate + sodium sulfite	470 / 605
[B] + [C]	(1) Tris(1,10-phenantroline)-ruthenium(II)-complex [RuPhe]	dissolved in sol-gel, tempered, dispersed in polystyrene	470 / 605
[B]	(2) Platinum(II) meso-tetra (pentafluorophenyl) porphine [PtPor]	dissolved in sol-gel + PMMA	505 / 630
[C]	(3) Ruthenium-tris-4,7-diphenyl-1,10-phenantroline [RuDiPh]	dissolved in PVC	470 / 605

Table I: Different temperature sensitive indicators with their matrices, the corresponding sensor configurations and the used excitation, λ_{ex}, and emission, λ_{em}, wavelengths, respectively.

1) The ruthenium phenantroline (RuPhe) complex was micellar dissolved in a solution of sodium dodecylsulfate [3]. This solution was kept oxygen free by adding the oxygen scavenger, sodium sulfite.
2) The same indicator, RuPhe, was dissolved in a sol-gel, that was tempered and grinded. The powder was then dispersed in polystyrene for immobilization on the fiber tip.
3) The Platinum porphine was dissolved in a mixture of a sol-gel and PMMA.
4) To use the weak permeability to oxygen of PVC, a ruthenium diphenyl phenatroline was dissolved in PVC.
All these approaches demanded their own ways of sensor realizations, that have been developed or adapted to existing preparation techniques [7-9].

2.2 Microoptodes

The temperature microoptodes consisted of a standard 100/140 µm multimode silica glass fiber with a standard ST-plug at one end. At the other end the protective PVC-tube and the plastic jacket were removed. The core and cladding were tapered down to a diameter of a few micrometers with a hot flame or in a light arc. The taper was cut to a diameter of 20 - 40 µm. Then three different configurations were realized (Fig. 1):

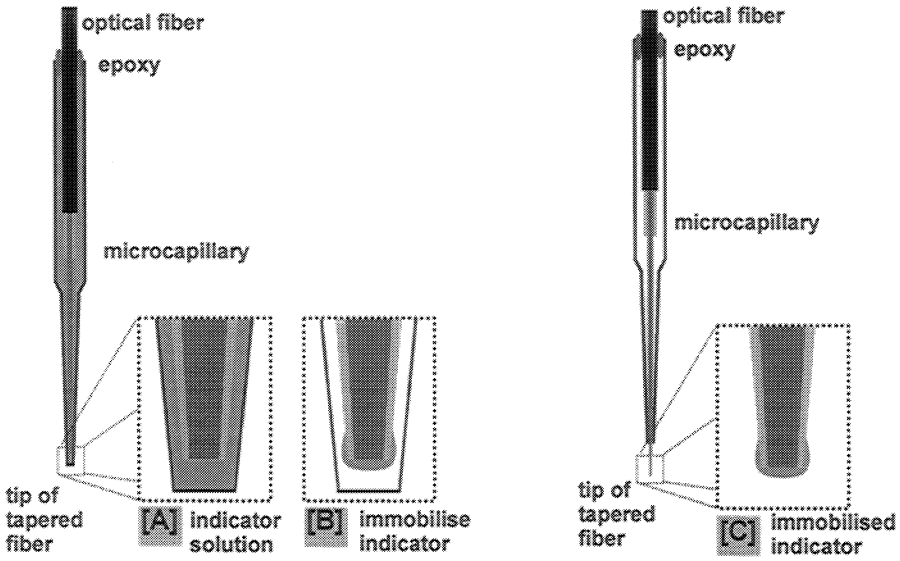

Figure 1: Schematic drawings of three different configurations for temperature microoptodes.

In the following we distinguish between (see figure 1):
Sensor type [A]:
The tapered fiber was introduced into a closed microcapillary that was also tapered to a tip diameter of appr. 30-50 µm. Then the capillary was filled with the oxygen free indicator solution (table I, indicator 1) under oxygen free conditions (nitrogen atmosphere) and finally closed and fixed with epoxy.
Sensor type [B]:
The tapered fiber was dip-coated with an indicator solution (table I, indicator 2+3). After evaporation of the solvent the fiber was introduced into a closed microcapillary that was tapered to a tip diameter of appr. 30-50 µm. This version was just filled with dry air, closed and fixed with epoxy.
Sensor type [C]:
The tapered fiber was dip-coated with an indicator solution (table I, indicator 2+4). After evaporation of the solvent the fiber was introduced into an open microcapillary. The fiber then was fixed at the two ends of the capillary with epoxy.
Because of the different indicators and the corresponding immobilization techniques the temperature sensitivity of the three configurations is different and sensor types [A] - [C] may exhibit different cross sensitivities.

3 Experiments and results

3.1 Calibration curves

Figure 2 shows the different calibrations curves of 4 different temperature microoptodes. The sensors were measured in a thermostatted water bath with a minimum immersion depth of 5 mm for each sensor. For a better comparison all curves were related to their initial lifetime value at 5 °C for each sensor.
The lifetimes were determined with a phase modulation technique [4, 5, 8, 9]. Using an apparent or average lifetime we measured at single modulation frequencies of 75 kHz (indicators 1,2 and 4) and 5 kHz (indicator 3). As excitation sources we used blue (λ_{peak} = 470nm, indicator 1, 2 and 4)) and blue-green LEDs (λ_{peak} = 505nm, indicator 3), and as detector a photomultiplier with a dual-phase-lock-in detection was used.
Although the calibration curves were not linear by nature in the interesting range of 5-45 °C we

reached for all calibration curves correlation coefficients better than 0.99 for linear regressions. The results are seen in table II. The most sensitive sensor configuration was the micellar ruthenium solution as sensor type [A], followed by the Platinum porphine in the airfilled microcapillary. The weakest temperature dependence was found for the ruthenium diphenyl PVC sensor (not drawn).

lifetime = a + b * temperature		
a [µs]	b [µs/°C]	curve
2.694	-0.0453	λ
2.414	-0.0203	ν
2.561	-0.0255	σ
45.533	-0.5762	τ

Table II: Linear regression results of calibrations curves.

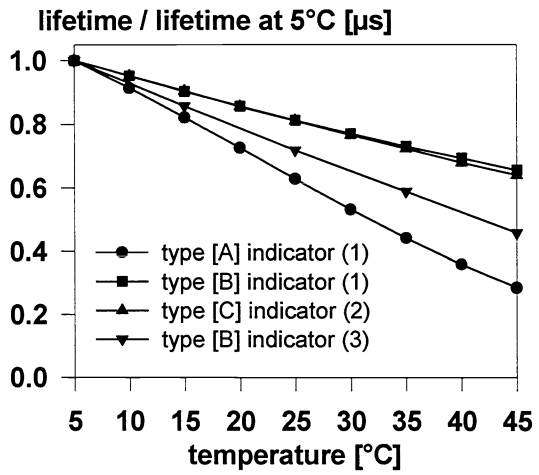

Figure 2: Calibration curves (lifetime vs. temperature for different sensor - indicator - combinations.

The closed and filled microcapillary sensors give rise to the question if and how temperature differences between the measuring volume in the tip and the big volume behind in the capillary influence the measurement. Additionally, it was necessary to investigate the cross sensitivity of sensors type [C] towards changes in oxygen concentration, that naturally occur in the investigated environments.

3.2 Cross Sensitivity towards temperature gradients along the sensor

To investigate the influence of temperature gradients along sensors type [A] and [B] the sensors were stepwise penetrated from air at room temperature (20 °C) into water at 5°C. The penetration depth was controlled by a pointer fixed to the sensor and a ruler in the millimeter range. Because of fluctuations on the water surface the precision of the surface position was +/- 1 mm.
As can be seen in figure 3 both sensors measure a temperature gradient above the water surface. After having penetrated the water, both signals stay constant. Although there is a large temperature difference between the part of the sensors outside and the measuring tip in the water, there was no effect on the measurements in the water. Strong axial temperature gradients thus seem to have only minor influence on the measuring signal of sensors type [A] and [B]. Nevertheless this experiment will be repeated with a setup that enables a better control of the spatial resolution e. g. the position of the border plane between the different temperatures.

3.3 Cross Sensitivity towards oxygen concentration

An eventual influence of oxygen on the temperature signal is only of importance for sensors type [C], because only this type of sensor has a direct contact to the environment. Sensors type [C] have not been investigated for the temperature difference along the sensor axis because their measuring volume is confined to the thin sensing layer on the fiber tip and can only be influenced by the poor heat conductivity of silica glass.
Sensors of type [C] were fixed in a calibration vessel (Fig. 4) filled with salt water and surrounded by thermostatted water at 25°C. The vessel was perfused by defined gas mixtures (air - 100% nitrogen -

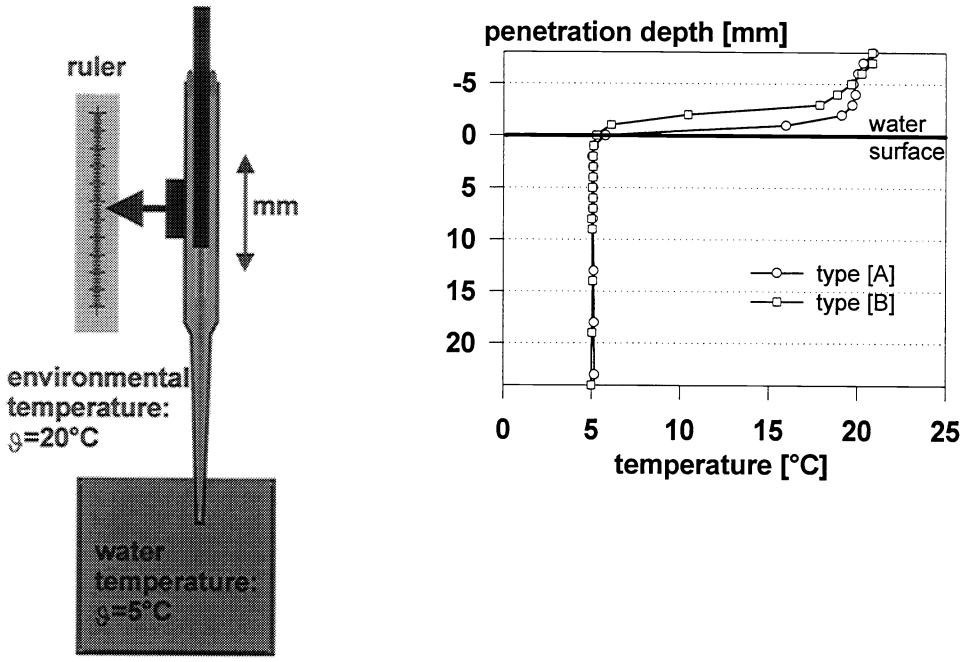

Figure 3: Schematic drawing of experimental setup for influence of temperature gradients along the sensor axis. The graph shows the results of measurements with sensors type [A] and [B].

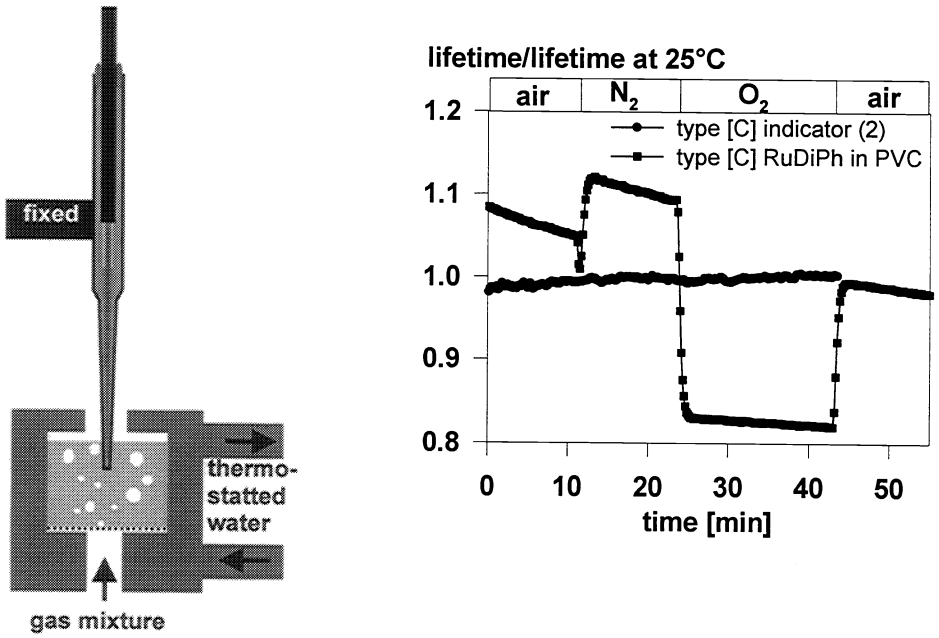

Figure 4: Schematic drawing of experimental setup for influence of oxygen concentration on the the measurement. The graph shows the results of measurements with sensors type [C].

100% oxygen - air). The results are given in in figure 4. For better comparison the lifetime recordings are related to their corresponding value at 25°C from the calibration curve. The RuDiPh sensor in PVC showed signal changes of > 10% when switching between air and nitrogen, or air and 100 % oxygen. The sol-gel sensor did not show any significant signal change as a function of the gas mixture applied.

3.3 Temperature depth profile

To demonstrate the application possibilities, we used a sensor type [A] for temperature measurements in a microbial mat sample from a hypersaline lake in Egypt. The mat was embedded in an agar layer, illuminated with a fiber-optic halogen light source and constantly flushed by a slow, nearly laminar flow of aerated salt water at 27 °C. The temperature microoptode was fixed to a micromanipulator and a depth profile was measured in steps of 100 - 500 µm (Fig. 5). The resulting profile clearly showed a temperature gradient in the water column above the mat that rises from 26.7 °C to 27.7 °C while approaching the mat surface. As the mat consisted of a dense light absorbing surface layer of cyanobacteria a slight temperature maximum was found here reaching 27.85 °C. Below the surface layer the mat temperature was constant at 27.75 °C.
Our results show temperature differences up to 1 °C to be present in illuminated microbial mats. The mechanism behind the temperature maximum in the surface layers and how it affects other microsensor measurements should be investigated in more detail. The presented temperature microoptodes are an important prerequisite for such further investigations.

3.4 Further developments

There are still some storage stability problems that have to be solved for the present sensors. For example it may happen in sensor type [A] that the oxygen scavenger sodium sulfite is consumed after a certain storage time and if the sensor was not prepared properly under oxygen free conditions (which is in fact very difficult to achieve) oxygen starts to equilibrate slowly with the surrounding air. This will lead to a change in the calibration curve, and the temperature sensitivity of the sensor will decrease. Another problem with sensors of type [B] can occur if the air inside the microcapillary is not dry. Then the measured oxygen will change with temperature and humidity. Additionally we need to optimize the optical filtering for sensors type [B] and [C] because there may be an additional noise signal. The blue excitation light may leave the sensor tip and can excite natural chlorophyll luminescence that interfers with the phase modulation signal.

4 Conclusion

The new temperature microoptodes open the possibility for temperature measurements in the biologically interesting range from 0-50 °C at a good thermal (0.25 °C) and a high spatial (<100 µm) resolution. If a high thermal resolution < 0.15 °C is needed, sensors type [A] and [B] with indicators (1) and (3) are best. If a fast response and a high spatial resolution < 40 µm is necessary, sensor type [C] with indicator (1) in sol-gel has advantages, although the temperature sensitivity is smaller.
The existing storage stability problems are currently investigated and the optical filtering concerning the influence of external luminescence will be improved.

5 Acknowledgments

We gratefully acknowledge the helpful discussions with Andrea Wieland and Eric Epping and the technical support of Vera Hübner. Financial support was due to EC MAST III project MICROMARE, No. MASCT950029 and the Red-Sea-Program, Project E - Microbial Activities in hypersaline interfaces controlling nutrient fluxes (German Ministery of Research and Development, BMBF).

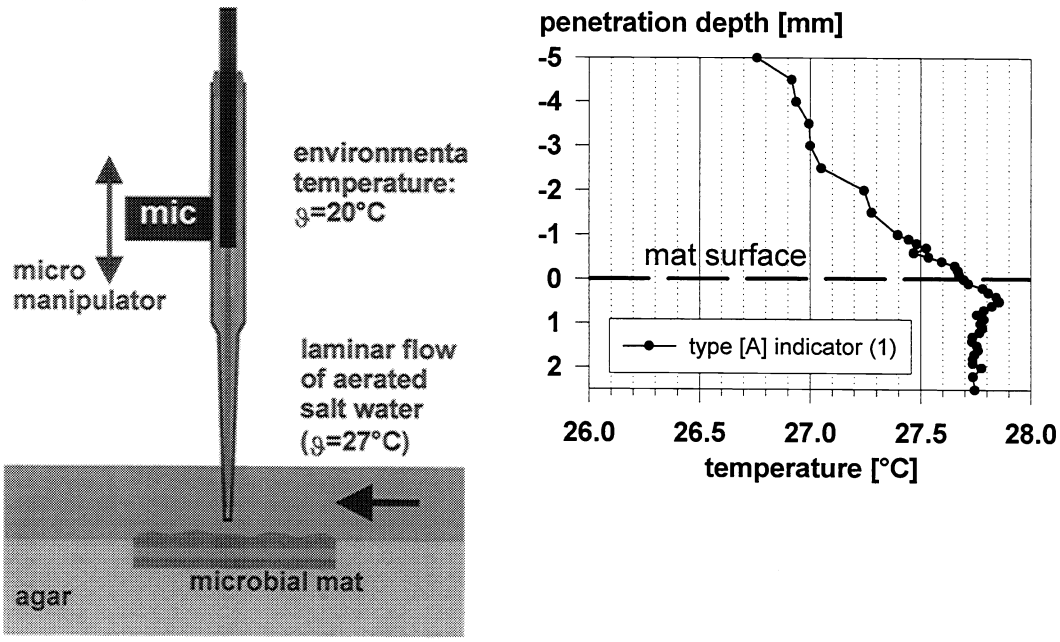

Figure 5: Schematic drawing of experimental setup for a temperature profile measurement in a microbial mat from a hypersaline lake (Solar Lake, Egypt). The graph shows the penetration depth vs. temperature result of a sensors type [A] with indicator (1).

6 References

1. J.N. Demas and B.A. DeGraff, „On the Design of Luminescence Based Temperature Sensors", SPIE Vol. 1796, pp. 71-75, 1992.

2. A. Juris, V. Balzani, S. Campagna, P. Belser and A. von Zewelsky, „Ru(II) Polypyridine Complexes: Photophysics, Photochemistry, Electrochemistry and Chemiluminescence", Coordination Chemistry Reviews, 84, pp.85-227, 1988.

3. B.L. Hauenstein (Jr.), W.J. Dressick, S.L. Buell, J.N. Demas and B.A. DeGraff, „A New Probe of Solvent Accessibility of Bound Photosensitizer. 1. Ruthenium (II) and Osmium (II) photosensitizers in Sodium Lauryl Sulfate Micelles", Journal of American Chemical Society, 105, pp. 4251-4255, 1983.

4. Z. Zhang, K.T.V. Grattan and A.W. Palmer, „Phase-Locked Detection of Fluorescence Lifetime", Review of Scientific Instrumentation, 64 (9), pp. 2531-2540, 1993.

5. J.R. Alcala, S.-C. Liao and J. Zheng, „Real Time Frequency Domain Fiberoptic Temperature Sensor", IEEE Transactions on Biomedical Engineering, 42 (5), pp. 471-476, 1995.

6. M. Brenci, G. Conforti, R. Falciai, A.G. Mignani and A.M. Scheggi, „All-Fiber Temperature Sensor", Journal of Optical Sensors, 1, pp. 163-169, 1986.

7. I. Klimant, V. Meyer and M. Kühl, „Fiber-Optic Oxygen Microsensors, a New Tool in Aquatic Biology", Limnology & Oceanography, 40, pp. 1159-1165, 1995.

8. G. Holst, M. Kühl and I. Klimant, „ A Novel Measuring System for Oxygen Microoptodes based on a Phase Modulation Technique", SPIE Vol. 2508, pp. 387-398, 1995.

9. G. Holst, R.N. Glud, M. Kühl and I. Klimant, „A Microoptode Array for Fine Scale Measurement of Oxygen Distribution", Sensors and Actuators B, (in press) 1996.

10. I. Klimant, M. Kühl, R.N. Glud and G. Holst, „Optical Measurement of Oxygen and Temperature in Microscale: Strategies and Biological Applications", Sensors and Actuators B, (in press), 1996.